SAE TECHNICAL
PAPER SERIES

2006-01-2334

Vision Performance Measures for Optimization-Based Posture Prediction

Timothy Marler, Kimberly Farrell, Joo Kim,
Salam Rahmatalla and Karim Abdel-Malek
Virtual Soldier Research (VSR) Program, University of Iowa

Digital Human Modeling for Design
and Engineering Conference
Lyon, France
July 4-6, 2006

SAE International™

400 Commonwealth Drive, Warrendale, PA 15096-0001 U.S.A. Tel: (724) 776-4841 Fax: (724) 776-0790 Web: www.sae.org

The Engineering Meetings Board has approved this paper for publication. It has successfully completed SAE's peer review process under the supervision of the session organizer. This process requires a minimum of three (3) reviews by industry experts.

ISSN 0148-7191

Printed in USA

2006-01-2334

Vision Performance Measures for Optimization-Based Posture Prediction

Timothy Marler, Kimberly Farrell, Joo Kim,
Salam Rahmatalla and Karim Abdel-Malek
Virtual Soldier Research (VSR) Program, University of Iowa

ABSTRACT

Although much work has been completed with modeling head-neck movements as well with studying the intricacies of vision and eye movements, relatively little research has been conducted involving how vision affects human upper-body posture. By leveraging *direct human optimized posture prediction* (D-HOPP), we are able to predict postures that incorporate one's tendency to actually look towards a workspace or see a target. D-HOPP is an optimization-based approach that functions in real time with Santos™, a new kind of virtual human with a high number of degrees-of-freedom and a highly realistic appearance. With this approach, human performance measures provide objective functions in an optimization problem that is solved just once for a given posture or task. We have developed two new performance measures: visual acuity and visual displacement. Although the visual-acuity performance measure is based on well-accepted published concepts, we find that it has little effect on the predicted posture when a target point is outside one's field of view. Consequently, we have developed visual displacement, which corrects this problem. In general, we find that vision alone does not govern posture. However, using multi-objective optimization, we combine visual acuity and visual displacement with other performance measures, to yield realistic and validated predicted human postures that incorporate vision.

INTRODUCTION

Virtual humans modeled on a computer have been used in the entertainment industry and are now providing a useful tool for engineering design, especially with respect to ergonomics. With avatars that act as real humans and provide feedback with respect to reach, comfort, physiology, joint torque, and other quantities, one can evaluate and modify digital prototypes without having to create more costly physical prototypes. Such a process can save money and time. In addition, virtual humans can be used not just for product design but also for studying the human body.

To a large extent, virtual humans have required an expert user to position or manipulate them. There are few virtual-human products with predictive capabilities. However, we have developed a new approach to posture prediction called the *direct human optimized posture prediction* (D-HOPP) approach. It affords the virtual human a substantial amount of predictive autonomy, enabling simulations that independently respond to infinitely many scenarios without any prerecorded data or manipulation of the avatar. With this approach, joint angles provide design variables for an optimization formulation that is solved just once for a predicted posture. The problem is constrained primarily by requiring a specified *end-effector* (i.e. a fingertip, elbow, etc.) to contact a specified point, line, or plane. An end-effector is a point of interest on a kinematic chain, and with this study, the end-effector is the tip of the index finger. Joint limits are imposed as constraints as well and are based on anthropometric data. Skeletal dimensions are also based on anthropometric data, so skeletal and joint characteristics are easily modified. Human performance measures that represent physically significant quantities, such as joint displacement, discomfort, etc., provide the objective functions, and multiple performance measures can be used concurrently by employing multi-objective optimization (MOO).

We contend that human posture is *task-based*, meaning posture is governed by different performance measures, depending on which task is being completed. However, some concepts are general enough that they apply to most scenarios. For instance, as suggested by Marler *et al* (2005a), people typically strive to see what they are touching or working with. That is, vision almost always affects some component of human posture, and it often affects portions of the skeletal system other than the eyes or neck. Some performance measures do not accurately predict posture when used independently; rather, they provide a critical ingredient to be combined with other more general performance measures using MOO (Marler *et al*, 2005b). This is the case with vision.

The primary goal of this paper is to develop performance measures for modeling the tendency to look at objects. The consequent posture prediction approach affects the complete skeletal system, not just the neck. However, the intent is not to model the specifics of site or even movement of the eye; the focus is on overall posture prediction. This work involves three main components: 1) modeling the neck and coordinating its motion with that of the torso and arms, 2) developing physics-based performance measures incorporating the line of site, and 3) aggregating vision with other performance measures using MOO. With respect to the first component, we leverage the optimization approach of D-HOPP, which naturally coordinates the motion of multiple limbs that depend on common degrees-of-freedom (DOFs) (i.e. the torso) as discussed by Farrell *et al* (2005). With respect to the second component, the intent is to model mathematically physically significant well-accepted characteristics or features, such as visual acuity. This effort progresses in three stages. First, visual acuity is modeled mathematically. Then, in response to observed deficiencies in this concept, the model is extended to represent what we call *visual displacement*. Finally, because we find that vision alone does not govern human posture, MOO is used to aggregate vision with an additional human performance measure.

Before presenting the details of the proposed performance measures, we present an overview of D-HOPP, including a description of the human model and an outline of the optimization formulation. Then, the models for visual acuity and visual displacement are discussed with their corresponding results. Finally, MOO results are discussed with which visual acuity and visual displacement are combined with joint displacement, and these final results are validated using motion-capture.

LITERATURE REVIEW

Although many researchers have studied the cervical spine (the neck), the details of vision, the nature of eye movement, and even various characteristics of eye-hand coordination, little work has been completed that incorporates the tendency to look at what one is working with, in posture-prediction models. In addition, many of the computational models for the neck, which is critical in modeling one's line of site, are relatively simple. Whereas Mi (2004) and Marler *et al* (2005a) provide extensive reviews of posture-prediction capabilities, here we present an overview of work with modeling the neck and the effects of vision on posture.

Much work has been completed that involves experimentation with neck motion and vision. For example, Yoganandan *et al* (1996) develop a dummy head-and-neck system for dynamic analysis and testing, and Humm *et al* (1999) use a similar system to conduct experiments to study the response of a head-and-neck system when impacted. DeSantis (2004) also develops a dummy head-and-neck system in an effort to reproduce experimental data. Andreoni *et al* (2004) use motion-capture with a proposed experimental methodology to study automobile accessibility and its relation to discomfort, contending that the head and neck motion plays a large role in dictating ingress and egress maneuvers.

Although many studies concerning the neck and vision are experimental, some work has been completed with modeling. This kind of work originated with vision-based control of robots, a survey of which is provided by Hashimoto (2003). Ouefelli *et al* (1999) solve a system identification problem to determine the kinematic characteristics of the neck model that most accurately approximates given data. However, the model has only three DOFs, which the authors determine is too few. With the intent of studying the neural control of the neck, Mitelman and Enderle (2001) develop a model based on the neck muscular system and its relationship with the central nervous system. Zanasi *et al* (2002) provide a basic 3-DOF planar dynamic model of the neck for studying passenger head movements in an automobile. Kim *et al* (2004b) model the neck and vision in the context of a method for coordinating multiple subsystems, such as visual gaze and manual reach. Essentially, and inverse-kinematics approach to seated motion prediction is extended to solve the subsystem of each limb separately. The subsystems consist of a 9-DOF manual subsystem, which includes the torso and right arm, and an 8-DOF visual subsystem, which includes the torso and neck. The neck itself is composed of five DOFs. With respect to modeling vision, conceptually, the line of site is simply constrained to intersect the point of interest. A weighted pseudo-inverse of the Jacobian is used, and the weights are set such that the predicted motion approximates prerecorded motion. Given an inverse kinematics solution for each subsystem, a secondary objective is applied to reconfigure the shared joint angles, which occur in the torso.

Many authors have studied movement of the actual eye. Yamada (1991) studies eye-head coordination and finds that it is almost impossible to rotate or translate the head without tilting one's neck. In addition, when visual targets move more than thirty degrees away from the line of site, one tends to move one's eyes more than the head. Crowley *et al* (1995) develop models for simulating how the eyes fixate on a point. Drawing on observations from psychology, human factors, and computer vision, Chopra-Khullar and Badler (1999), and Gillies and Dodgson (2002) provide computational frameworks for modeling how an avatar reacts, in terms of eye movement, to the viewed or peripheral environment.

OVERVIEW OF D-HOPP

In this section, we provide an overview of D-HOPP. This includes a brief description of the skeletal model including the neck, an overview of our approach for coordinating multiple limbs with shared DOFs, and the final optimization formulation.

Simulating human posture depends largely on how the human skeleton is modeled. We view a skeleton as a kinematic system, a series of links with each pair of links connected by one or more revolute joints. Therefore, a complete human body can be modeled as several kinematic chains, formed by series of links and revolute joints, as shown in Figure 1.

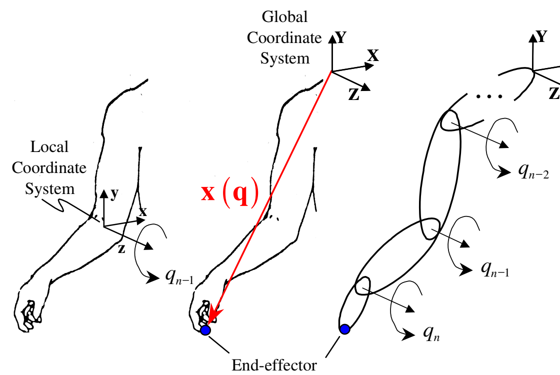

Figure 1: A Kinematic Chain of Joints

q_i is a *joint angle* and represents the rotation of a single revolute joint. There is one joint angle for each DOF. $\mathbf{q} = [q_1, \ldots, q_n]^T \in R^n$ is the vector of joint angles in an *n*-DOF model and represents a specific posture. Each skeletal joint is modeled using one, two, or three kinematic revolute joints. $\mathbf{x}(\mathbf{q}) \in R^3$ is the position vector in Cartesian space that describes the location of the end-effector as a function of the joint angles, with respect to the global coordinate system. For a given set of joint angles $\mathbf{q}$, $\mathbf{x}(\mathbf{q})$ is determined using the Denavit-Hartenberg (DH)-method (Denavit and Hartenberg, 1955).

Using the DH-method $\mathbf{x}(\mathbf{q})$ is expressed in terms of transformations ${}^{i-1}\mathbf{T}_i$ and is given by:

$$\mathbf{x}(\mathbf{q}) = \left(\prod_{i=1}^{n} {}^{i-1}\mathbf{T}_i \right) \mathbf{x}_n \tag{1}$$

$$ {}^{i-1}\mathbf{T}_i = \begin{pmatrix} \cos\theta_i & -\cos\alpha_i \sin\theta_i & \sin\alpha_i \sin\theta_i & a_i \cos\theta_i \\ \sin\theta_i & \cos\alpha_i \cos\theta_i & -\sin\alpha_i \cos\theta_i & a_i \sin\theta_i \\ 0 & \sin\alpha_i & \cos\alpha_i & d_i \\ 0 & 0 & 0 & 1 \end{pmatrix} \tag{2}$$

where $\mathbf{x}_n$ is the position of the end-effector with respect to the n^{th} frame and *n* is the number of DOFs. Note that the rotational displacement q_i changes the value of θ_i.

With this study, a 26-DOF model for the human torso, right arm, and neck is used and is shown in Figure 2, where each cylinder represents a rotational DOF.

q_1 through q_{12} represent the torso. q_{13} through q_{17} represent the shoulder and clavicle. q_{18} through q_{21} represent the right arm. q_{22} through q_{30} represent the left arm, which is not shown in this study. q_{31} through q_{35} represent the 5-DOF neck model. The link lengths between each of the joints are variable and can be set based on anthropometric data, thus representing various population variations.

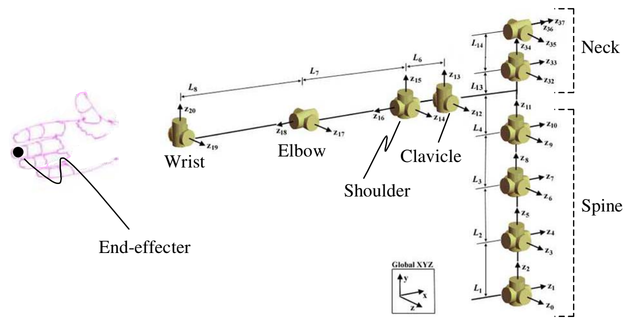

Figure 2: 26-DOF Kinematic Model

MULTIPLE-LIMB COORDINATION

Although there is an increasing demand for predicting human postures in real time, there has been minimal progress with methods that can incorporate multiple limbs with shared DOFs. However, D-HOPP provides an elegant and robust solution to the problem of multiple-limb coordination. This new approach also easily extends to models with a higher number of DOFs and additional end-effectors. Here, we present an overview of this approach, while Farrell *et al* (2005) give details.

With Santos's™ upper body, there are essentially three limbs: the neck and two arms. Therefore, there are three end-effectors. In addition, there are twelve shared DOFs in the torso. For modeling multiple limbs, it is possible to compute the position of the end-effector of each chain separately using (1) and (2). However, the transformations for the shared DOFs need only be calculated once. In general, the position $\mathbf{x}_{\text{limb}}(\mathbf{q})$ of a given limb's end-effector can be calculated by:

$$\mathbf{x}_{\text{limb}}(\mathbf{q}) = (\mathbf{T}_{\text{shared}})(\mathbf{T}_{\text{transform}})(\mathbf{T}_{\text{limb}})\mathbf{x}_n \tag{3}$$

where $\mathbf{T}_{\text{shared}}$ is the transformation matrix describing the position and orientation of the last shared coordinate frame with respect to the global coordinate system. $\mathbf{T}_{\text{transform}}$ describes the position and orientation of the first coordinate frame of the limb with respect to the last shared coordinate frame. $\mathbf{T}_{\text{limb}}$ describes the position and orientation of the last coordinate frame of the limb with respect to the first coordinate frame of the limb. These transformations are depicted in Figure 3.

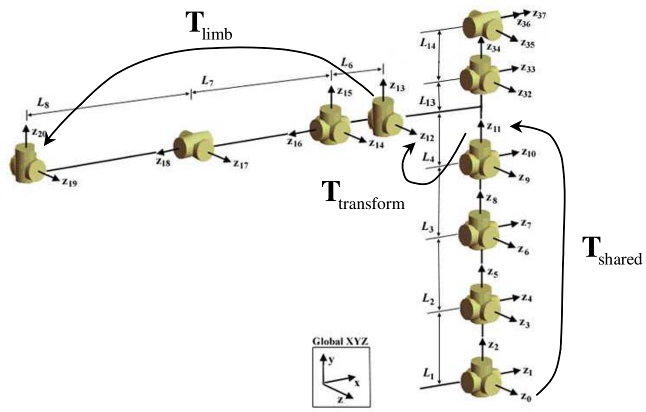

Figure 3: The transformation matrices

OPTIMIZATION FORMULATION

The posture of the above-described model is determined by solving the optimization problem formulated in this section. The design variables for the problem are q_i, measured in units of radians. The vector $\mathbf{q}$ represents the consequent posture.

The first constraint, called the *distance* constraint, requires the end-effector to contact a target point. In addition, each joint angle is constrained to lie within predetermined limits. q_i^U represents the upper limit for q_i, and q_i^L represents the lower limit. These limits are derived from anthropometric data and ensure that the avatar does not assume an unrealistic posture.

The basic benchmark performance measure represents joint displacement (Jung *et al*, 1994; Yu, 2001; Mi *et al*, 2002). This performance measure is proportional to the deviation from the *neutral position*, which is selected as a relatively comfortable posture, typically a standing position with arms at one's sides. q_i^N is the neutral position of a joint, and $\mathbf{q}^N$ represents the overall posture. Because some joints articulate more readily than others, a weight w_i is introduced to stress the relative stiffness of a joint. Although these weights are typically based on trial-and-error, the consequent performance measure provides a documented benchmark for the development of new performance measures. The final joint displacement is given as follows:

$$f_{JointDisplacement}(\mathbf{q}) = \sum_{i=1}^{n} w_i \left(q_i - q_i^N\right)^2 \tag{4}$$

The optimum posture for the system shown in Figure 2 is then determined by solving the following problem:

Find: $\mathbf{q} \in R^{DOF}$ (5)

to minimize: $f_{JointDisplacement}(\mathbf{q})$

subject to: $distance = \left\| \mathbf{x}(\mathbf{q})^{end\text{-}effector} - \mathbf{x}^{target\ point} \right\| \leq \varepsilon$

$$q_i^L \leq q_i \leq q_i^U;\ i = 1, 2, \ldots, DOF$$

where ε is a small positive number that approximates zero. (5) is solved using the software SNOPT (Gill *et al*, 2002), which uses a sequential quadratic programming algorithm. Analytical gradients are determined for the objective function and for all constraints. Note that the absolute values of eth performance measures are not significant. For instance, it means little to suggest that joint displacement has a value of 2. However, the relative change in the performance measures (between different postures) is significant.

VISUAL ACUITY

PERFORMANCE-MEASURE DEVELOPMENT

Given the construct of the D-HOPP optimization formulation, we now describe the performance measures for vision. Because the main focus is posture prediction, the goal is to model components of vision that affect overall body posture, although eye movement is not yet considered.

One such component is *visual acuity*. By definition, visual acuity is the capacity to discriminate the fine details of objects in eth field of view (Graham *et al*, 1965). It is the clearness of vision, dependent primarily on the sharpness of focus. Acuity can depend on age, luminance, and linear distance, but most relevant to overall posture is its inverse dependence on the angular distance from the eye fovea. This is because the density of cone photoreceptors in the retina decreases with distance from the fovea. Thus, as a visual target moves further from the fovea, visual acuity (the clarity of the viewed target) drops until it reaches zero when the target is outside one's field of peripheral vision, as shown in Figure 4.

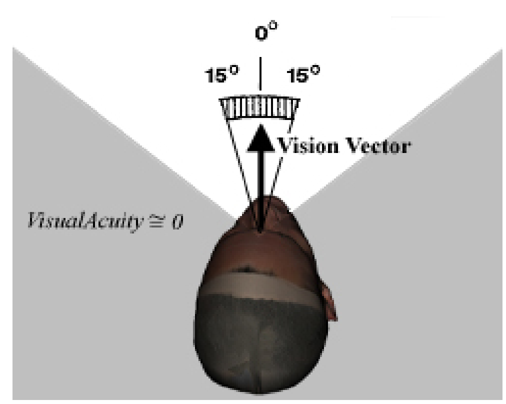

Figure 4: Schematic of visual acuity

Consequently, one generally strives to minimize the angular distance between the line of site and a visual target. This aspect of visual acuity, which drives one to align with a target in order to increase clarity, is called *relative visual acuity*. In order to model relative acuity, we represent the angular distance with what we call the *site angle*. The site angle is the angle between the vector from the eye to the target (eye-to-target vector), and the *vision vector*, which emanates from the eye perpendicular to the face. Relative to the site angle, visual acuity has a maximum value of one when the angle is approximately zero, and it decreases exponentially as the site angle increases.

Kim *et al* (2004a) derives the following formula for relative visual acuity by interpolating published data (Coren *et al*, 1978; Sekular abd Blake, 1985; Plotnick *et al*, 1998; Blanke and Baja, 2002):

$$VisualAcuity = e^{-7|\theta(\mathbf{q})|} \qquad (6)$$

θ is the site angle and is a function of the joint variables $\mathbf{q}$. It is determined using the arc cosine of the dot product between the vision vector and the eye-to-target vector. Note that the precise details of the relationship between relative acuity and the angle from the fovea vary slightly depending on the source, but the general trend is consistent throughout the literature.

Although (6) is a realistic model of visual acuity, because of the arc cosine term, the gradient is undefined when the dot product is one (when $\theta(\mathbf{q})=0$). Such discontinuities can cause difficulties with gradient-based optimization routines, such as the one used with D-HOPP. To avoid these discontinuities, we approximate (6) by replacing $|\theta(\mathbf{q})|$ with $n(1-\cos(\theta))$. Then, to determine the most appropriate value for *n*, we constrain the proposed visual acuity performance measure $f_{VisualAcuity}$ such that it is equal to the expression in (6) at a point (a value for theta) where the curve is diagonal. Thus, we set $f_{VisualAcuity}(0.4) = VisualAcuity(0.4)$ and find that $n=5$. The consequent expression is given as follows:

$$f_{VisualAcuity} = e^{-35[1-\cos(\theta(\mathbf{q}))]} \qquad (7)$$

where $\cos(\theta)$ is calculated using the dot product.

The proposed visual acuity in (7) is plotted against the visual acuity model of (6) and is shown in Figure 5. Figure 5 shows that (7) provides an accurate representation of relative visual acuity while maintaining continuity.

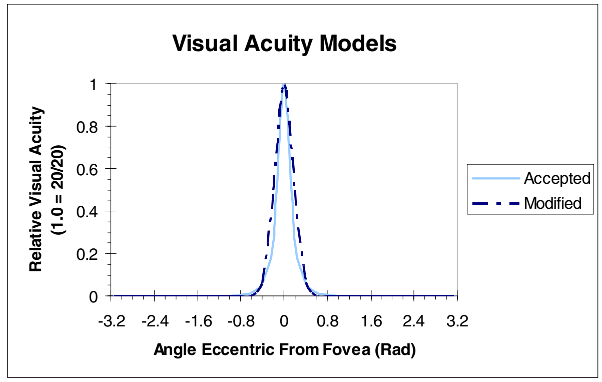

Figure 5: Published and proposed visual acuity models

However, this proposed visual acuity must be maximized, whereas the formulation in (5) is used to minimize the objective function (performance measure). Therefore, the final model is given as follows and is minimized:

$$f_{VisualAcuity}(\mathbf{q}) = -e^{-35(1-\cos[\theta(\mathbf{q})])}+1 \qquad (8)$$

(8) is inherently normalized such that $f_{VisualAcuity}(\mathbf{q}) \in [0,1]$. Note that values for relative visual acuity are reported based on (7), where a value of 1.0 indicates a high visual acuity.

RESULTS

Using visual acuity from (8) results in the posture shown in Figure 6. Alternatively, using joint displacement from (4) results in the posture shown in Figure 7. Target 1 is located at $(-50,31,47)$ relative to the first torso joint in Figures 2 and 3, where coordinates are given in units of cm.

Figure 6: Using visual acuity with Target 1 (joint displacement=148.58; visual acuity=1.00; visual displacement=0.00)

Figure 7: Using joint displacement with Target 1 (joint displacement=1.96; visual acuity=0.00; visual displacement=2.03)

Clearly, when visual acuity is used, Santos™ aligns his vision vector with the eye-to-target vector, and thus sees the target and assumes a more realistic posture. However, with target points where the angle between the vision vector and the eye-to-target vector is too great (the target is not within the field of peripheral vision), it is not possible to reduce the value of visual acuity. This is because the function is flat and the gradient has a constant value of zero. Consequently, targets that are difficult to see result in postures that are unrealistic, as shown in Figure 8, where visual acuity has a value of 0.00. Target 2 is located at $(-35,42,-30)$. We find that modeling visual acuity does not always accurately predict one's tendency to see a specified target.

Figure 8: Unsuccessful use of visual acuity with target 2 (joint displacement=193.84; visual acuity=0.00; visual displacement=9.09)

VISUAL DISPLACEMENT

PERFORMANCE-MEASURE DEVELOPMENT

In response to the results with visual acuity, we develop a new human performance measure based on the visual angle: *visual displacement*. Conceptually, we define visual displacement as the absolute value of the site angle no matter where the target point is located. Therefore, minimizing visual displacement essentially minimizes the site angle. That is, the further the visual angle is from zero, the higher the value of the visual displacement function. This idea is formulated mathematically as what we call basic visual displacement:

$$VisualDisplacment = \theta(\mathbf{q})^2 \tag{9}$$

where the site angle θ is obtained using arc cosine of the vector dot product. The concept of visual displacement is shown in Figure 9, as compared to Figure 4.

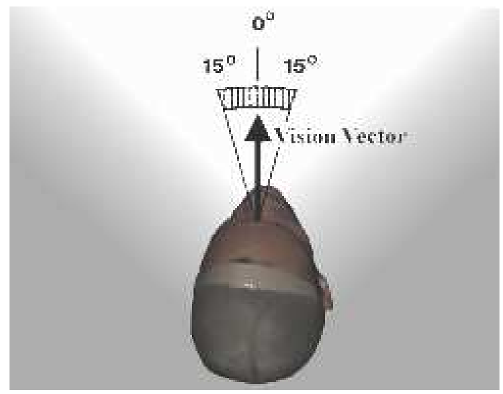

Figure 9: Schematic of visual displacement

However, as with acuity, because of the arc cosine term necessary to find θ, (9) is discontinuous. To avoid this discontinuity, the following expression is proposed:

$$f_{VisualDisplacement}(\mathbf{q}) = n\left(1-\cos\left[\frac{\theta(\mathbf{q})}{2}\right]\right) \tag{10}$$

This expression has the same basic conceptual significance and same mathematical properties as (9) but avoids the discontinuities. Using a similar approach as in (7), the value of *n* is determined by solving the following equality:

$$f_{VisualDisplacement}(\pi) = VisualDisplacement(\pi) \tag{11}$$

This results in $n=10$. In Figure 10, the basic formulation of (9) is plotted along with the proposed formulation of (10). The term $\cos(\theta/2)$ is calculated as the dot product between the normalized vision vector and the normalized sum of the vision vector and eye-to-target vector.

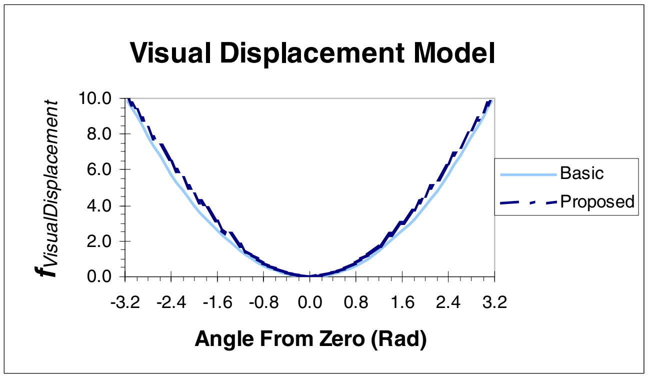

Figure 10: Basic and proposed visual displacement models

RESULTS

Figure 11 shows a posture obtained by using visual displacement as the performance measure. In this case, the target is the same as that in Figures 6 and 7. Figure 12 shows a posture obtained by using visual displacement, with the same target point that is used in Figure 8.

Figure 11: Using visual displacement with Target 1 (joint displacement=158.75; visual acuity=1.00; visual displacement=0.00)

Figure 12: Using visual displacement with Target 2 (joint displacement=232.83; visual acuity=0.05; visual displacement=0.84)

Note that in Figure 12, visual displacement does not have a value of 0.00 because of limits on the joints, which prohibit perfect alignment between the vision vector and the eye-to-target vector. Nonetheless, visual displacement resolves the difficulty that was experiences with visual acuity; with visual displacement, the avatar actually tries to look at the target point regardless of its location. Using visual displacement, we find that with targets far behind Santos^{TM}, there is a noticeable amount of head tilting, as suggested by Yamada (1991).

Although Figure 12 demonstrates that posture is affected by one's tendency to look at the target, it does not illustrate a particularly realistic posture. Additional examples of this condition are shown in Figures 13 and 14, where Target 3 is located at $(-43, 34, 34)$ and Target 4 is located at $(-26, -31, -8)$.

Figure 13: Using visual acuity with Target 3 (joint displacement=216.85; visual acuity=1.00; visual displacement=0.00)

Figure 14: Using visual displacement with Target 4 (joint displacement=141.99; visual acuity=1.00; visual displacement=0.00)

However, this is not an indication of poor results with respect to the overall approach. Conceptually, it simply suggests that vision alone does not necessarily govern human posture. Technically, the arms do not affect the vision vector or the eye-to-target vector. Therefore, the design variables used to represent the posture of the arms are not incorporated in the performance measure. In terms of the optimization formulation, this means the final solution for the values of the arm joint angles needs only be feasible, not optimal. This in turn suggests the need for combining vision with additional performance measures using MOO.

MULTI-OBJECTIVE OPTIMIZATION

MOO is a subfield of optimization that addresses the issue of how one considers multiple objective functions simultaneously. There are many methods for aggregating objectives and articulating preferences as to which objectives are more important (Marler and Arora, 2004). However, the goal of this work is to demonstrate our approach to modeling vision. Therefore, in terms of MOO methods, we use the following global criterion, based on work by Marler (2005):

$$F(\mathbf{q}) = \left\{ \left[w_1 \left(\frac{f_{Vision}}{f_{Vision}^{Max}} \right) + 1 \right]^2 + \left[w_2 \left(\frac{f_{JointDisplacement}}{f_{JointDisplacement}^{Max}} \right) + 1 \right]^2 \right\}^{\frac{1}{2}} \quad (12)$$

f_{Vision} represents either visual acuity or visual displacement. A superscript of *Max* indicates the maximum possible value for the performance measure. Note that the maximum value of a performance measure depends on the target point and the distance constraint in (5). Thus, in this case, the maxima are determined analytically considering the complete reach envelop (all target points). w_1 and w_2 are weights representing the relative importance of the two performance measures. In this case, $w_1 = 1.0$, and $w_2 = 1.0$. Ultimately, weights like these can be altered to model different kinds of behavior or to simulate postures associated with different kinds of tasks.

Figure 15 shows the posture resulting from the combination of visual acuity and joint displacement, along with results from motion-capture. Motion-capture results are indicated by the avatar with the solid colored cap. With Targets 3 and 4 (Figures 13 through 16), the link lengths in the avatar have been altered from default settings to reflect the characteristics of the motion-capture subject. The target point is dictated by the end-effector (tip of the middle finger) position given by the motion-capture results. That is, the target point is positioned based on experimental data. The consequent predicted posture is then compared to the posture based on experimental data. Clearly, the results in Figure 15 are much more realistic than those shown in Figure 13, where visual acuity is used independently. In addition, the motion-capture results validate the predicted posture.

Figure 16 shows the results when visual displacement is combined with joint displacement, again with motion-capture results. Considering the twist in the arm and the articulation of the clavicle, the results are more realistic than those shown in Figure 14, where visual displacement is used independently. Note that in Figures 15 and 16, the values for joint displacement are reduced significantly when compared to the values for Figures 13 and 14. This is an advantage of using MOO. There is a difference between the motion-capture results and the predicted posture, and considering the nature of the vision model, this provides insight into the way people move the way they do. Currently, the posture-prediction model does not incorporate movement in the eyes, and the results in Figure 16 suggest that in cases where postures become more uncomfortable, eye movement becomes more critical.

Figure 15: Aggregating visual acuity and joint displacement (joint displacement=2.44; visual acuity=1.00; visual displacement=0.00)

Figure 16: Aggregating visual displacement and joint displacement (joint displacement=29.26; visual acuity=0.95; visual displacement=0.01)

CONCLUSION

In this paper, we have introduced two new human performance measures for optimization-based posture prediction. Visual acuity is based directly on published data, while visual displacement is an extension of visual acuity and more accurately models one's tendency to look at a target or workspace. In developing these performance measures, we capitalized on the advantages of D-HOPP with respect to studying human posture and with respect to modeling multiple limbs that depend on shared DOFs.

We have advanced the D-HOPP approach and its ability to predict human posture accurately. However, we have also used D-HOPP to study how and why humans move the way they do. Visual acuity only takes into effect the tendency to look directly at an object that is already visible, and our model reflects this. In fact, using visual acuity generally provides more realistic results than visual displacement when the target is in Santos's™ initial field of view. However, we find that in addition to maximizing acuity, humans strive to see what may not initially be visible, and visual displacement takes this into consideration. Further, we find that vision alone does not govern human posture; rather, it provides a valuable component of the final performance measure.

Along these lines, the vision performance measures do not incorporate certain facets of neck movement, while joint displacement does. Generally, the vision performance measures model the tendency to assume a posture that makes it as easy as possible to look directly at an object. This does incorporate the tendency to keep one's head level, which can be a critical factor when predicting postures that involve looking behind one's self. However, by means of the relative values for the weights in (4), joint displacement does incorporate the tendency to avoid extensive neck rotation in the coronal plane.

As a proof of concept for the vision performance measures, this study involves only upper body posture prediction. In fact, Santos™ can perform lower-body posture prediction as well. Incorporating whole-body motion, where posture-prediction incorporates not just limb and torso motion, but also translation and rotation of the hip, is the final stage of posture-prediction development and is currently work in progress.

Validation generally occurs in three stages: 1) subjective validation, 2) basic motion-capture studies with a limited number of subjects for visual comparison, and 3) extensive motion-capture studies with a large number of subjects and statistical analysis. With this study, we have completed the first two phases in order to verify that our approach is valid. More extensive motion-capture studies are in progress. Note that given a non-specific task, such as simply touching a target point, there can be substantial variability in the posture that an individual or group of individuals assumes. Thus, for such tasks, there is no advantage to validating the precise value of specific joint angles. Rather, we simply validate the predicted posture strategy.

As a final topic for future work, it is necessary to incorporate actual eye movement. The focus with this work has been on the gross movement of the skeletal structure. Indeed, eye movement can affect the nuances of posture. Because the eyes are assumed fixed, in some cases the head/neck movement is overstated. Incorporating eye movement will likely involve vertical and horizontal threshold gaze angles that define the point at which head-neck movement tends to dominate eye movement.

ACKNOWLEDGMENTS

This research is funded by the US Army TACOM project: Digital Humans and Virtual Reality for Future Combat Systems (FCS), and the Caterpillar project: Digital Human Modeling and Simulation for Safety and Serviceability.

REFERENCES

1. Andreoni, G., Rabuffetti, M., and Pedotti, A. (2004), "Kinematics of Head-Trunk Movements while Entering and Exiting a Car," *Ergonomics*, 47 (3), 343-359.
2. Blanke, W., Bajaj, C. (2002), "Active Visualization in a Multidisplay Immersive Environment," *Eurographics Workshop on Virtual Environments*, May, Barcelona, Spain, Association for Computing Machinery, New York, 103-220.
3. Chopra-Khullar, S., and Badler, N. I. (1999), "Where to Look? Automating Attending Behaviors of Virtual Human Characters," *Proceedings of the Third International Conference on Autonomous Agents*, May, Seattle, WA, Association for Computing Machinery, New York, 16-23.
4. Coren, S., Porac, C., and Ward, L. M. (1978), *Sensation and Perception*, Academic Press, New York.
5. Crowley, J. L., Mesrabi, M., and Chaumette, F. (1995), "Comparison of Kinematic and Visual Servoing for Fixation," *Journal of Engineering and Applied Science*, 1, 335-341.
6. Denavit, J., and Hartenberg, R. S. (1955), "A Kinematic Notation for Lower-Pair Mechanisms Based on Matrices," *Journal of Applied Mechanics*, 22, 215-221.
7. DeSantis, K. (2004), "Development of an Improved Multi-Directional Neck Prototype," *Proceedings of the 35th Stapp Car Crash Conference*, November, San Diego, CA, Society of Automotive Engineers, Warrendale, PA, 2081-2092.
8. Farrell, K., Marler, R. T., and Abdel-Malek, K. (2005), "Modeling Dual-Arm Coordination for Posture: An Optimization-Based Approach," *SAE Human Modeling for Design and Engineering*

Conference, June, Iowa City, IA, Society of Automotive Engineers, Warrendale, PA.

9. Gill, P., Murray, W., and Saunders, A. (2002), "SNOPT: An SQP Algorithm for Large-Scale Constrained Optimization," *SIAM Journal of Optimization*, 12 (4), 979-1006.
10. Gillies, M. F., and Dodgson, N. A. (2002), "Eye Movements and Attention for Behavioural Animation," *The Journal of Visualization and Computer Animation*, 287-300.
11. Graham, C. H., Barlett, N. R., Brown, J. L., Hsia, Y., Mueller, C. G., and Riggs, L. A. (1965), *Vision and Visual Perception*, John Wiley and Sons, New York.
12. Hashimoto, K. (2003), "A Review on Vision-Based Control of Robot Manipulators," *Advanced Robotics*, 17 (10), 969-991.
13. Humm, J. R., Harris, G. F., Yoganandan, N., Mugnier, C. J., and Anderson, R. A. (1999), "Head and Neck Kinematics During Impact Loading," *Proceedings of the First Joint BMES/EMBS Conference: Serving Humanity, Advancing Technology*, October, Atlanta, GA, Institute of Electrical and Electronics Engineers, Piscataway, NJ, 518.
14. Jung, E. S., Choe, J., and Kim, S. H. (1994), "Psychophysical Cost Function of Joint Movement for Arm Reach Posture Prediction," *Proceedings of the Human Factors and Ergonomics Society 38th Annual Meeting*, October, Nashville, TN, Human Factors and Ergonomics Society, Santa Monica, CA, 636-640.
15. Kim J., Abdel-Malek, K., Mi, Z., and Nebel, K. (2004a), "Layout Design Using an Optimization-based Human Energy Consumption Formulation," *SAE Digital Human Modeling for Design and Engineering Conference*, June, Society of Automotive Engineers, Warrendale, PA.
16. Kim, K. H., Martin, B. J., and Gillespie, R. B. (2004b), "Modeling the Coordinated Movements of the Head and Hand Using Differential Inverse Kinematics," *Proceedings of the SAE Digital Human Modeling for Design and Engineering*, Oakland, June, MI.
17. Marler, R. T. (2005), "A Study of Multi-objective Optimization Methods for Engineering Applications," Ph.D. Dissertation, University of Iowa, Iowa City, IA.
18. Marler, R. T., and Arora, J. S. (2004), "Survey of Multi-Objective Optimization Methods for Engineering," *Structural and Multidisciplinary Optimization*, 26 (6), 369-395.
19. Marler, R. T., Rahmatalla, S., and Shanahan, M., and Abdel-Malek, K. (2005a), "A New Discomfort Function for Optimization-Based Posture Prediction," *SAE Human Modeling for Design and Engineering Conference*, June, Iowa City, IA, Society of Automotive Engineers, Warrendale, PA.
20. Marler, R. T., Yang, J., Arora, J. S., and Abdel-Malek, K. (2005b), "Study of Bi-Criterion Upper Body Posture Prediction using Pareto Optimal Sets," *IASTED International Conference on Modeling, Simulation, and Optimization*, August, Oranjestad, Aruba, International Association of Science and Technology for Development, Canada.
21. Mi, Z. (2004), "Task-Based Prediction of Upper Body Motion," Ph.D. Dissertation, University of Iowa, Iowa City, IA.
22. Mi, Z., Yang, J., Abdel-Malek, K., Mun, J. H., and Nebel, K. (2002), "Real-Time Inverse Kinematics for Humans," *Proceedings of the 2002 ASME Design Engineering Technical Conferences and Computer and Information in Engineering Conference*, 5A, September, Montreal, Canada, American Society of Mechanical Engineers, New York, 349-359.
23. Mitelman, Y., and Enderle, J. (2001), "Building a Mathematical Model of the Head-Neck System; Modeling and Simulation of the 6-Degree of Freedom Head Movement," *Proceedings of the IEEE 27th Annual Northeast Bioengineering Conference*, April, Storrs, CN, Institute of Electrical and Electronics Engineers, Piscataway, NJ, 81-82.
24. Ouerfelli, M., Kumar, V., and Harwin, W. S. (1999), "Kinematic Modeling of Head-Neck Movements," *IEEE Transactions on Systems, Man, and Cybernetics – Part A: Systems and Humans*, 29 (6), 604-615.
25. Plotnick, M., Kinoshita, T., Yoshigi, H., and Kageyama, M. (1998), "High-Quality Bit-rate Transformation for the Home Media Station," *IEEE Transactions on Consumer Electronics*, 44 (3), 587-590.
26. Sekuler, R. (2002), *Perception*, McGraw-Hill, New York.
27. Yamada, M. (1991), "Eye-Head Coordination while Viewing a Target on a Two-Dimensional Plane," *Proceedings of the Annual International Conference on the IEEE Engineering in Medicine and Biology Society*, November, Orlando, FL, Institute of Electrical and Electronics Engineers, Piscataway, NJ, 2159-2161.
28. Yoganandan, N., Cheng, J., Pintar, F. A., Shams, T., and Rangarajan, N. (1996), "Hybrid Approach to the Biomechanical Design of a Dummy Human Neck," *Proceedings of the 1996 ASME International Mechanical Engineering Congress and Exposition*, November, Atlanta, GA, American Society of Mechanical Engineers, New York, 449-450.
29. Yu, W. (2001), *Optimal Placement of Serial Manipulators*, Ph.D. Dissertation, University of Iowa, Iowa City, IA.
30. Zanasi, R., Morselli, R., Visconti, A., and Cavanna, M. (2002), "Head-Neck Model for the Evaluation of Passenger's Comfort," *Proceedings of the 2002 IEE/RSJ International Conference on Intelligent Robots and Systems*, October, Lausanne, Switzerland, Institute of Electrical and Electronics Engineers, Piscataway, NJ, 1403-1408.